arXiv:astro-ph/0002442v1 23 Feb 2000

Physics in Ultra-strong Magnetic Fields

Robert C. Duncan

Dept. of Astronomy and McDonald Observatory
University of Texas at Austin

Abstract. In magnetic fields stronger than $B_Q \equiv m_e^2 c^3/\hbar e = 4.4 \times 10^{13}$ Gauss, an electron's Landau excitation energy exceeds its rest energy. I review the physics of this strange regime and some of its implications for the crusts and magnetospheres of neutron stars. In particular, I describe how ultra-strong fields

- render the vacuum *birefringent* and capable of distorting and magnifying images ("magnetic lensing");
- change the self-energy of electrons: as B increases they are first slightly lighter than m_e, then slightly heavier;
- cause photons to rapidly split and merge with each other;
- distort atoms into long, thin cylinders and molecules into strong, polymer-like chains;
- enhance the pair density in thermal pair-photon gases;
- strongly suppress photon-electron scattering, and
- drive the vacuum itself unstable, at extremely large B.

In a concluding section, I discuss the spindown of ultra-magnetized neutron stars and recent soft gamma repeater observations.

ELECTRONS AT $B > B_Q$

The significance of the quantum electrodynamic field strength, B_Q, can be understood via a simple, semi-classical argument. A classical electron gyrating in a magnetic field satisfies $\dot{p} = ev \times B/c$, where $p = \gamma m_e v$ is the momentum. Substituting $\dot{p} = \omega p$ and $v = \omega r$ in this equation and cancelling factors of ω (along with orbital phase factors), one finds a radius of gyration $r = cp/eB$, where p is the transverse momentum ($\perp \mathbf{B}$). Quantum mechanics implies $r \cdot p \sim \hbar$ in the ground state, thus the semi-classical gyration radius is $r_{\rm gyr} \sim \lambda_e \, (B/B_Q)^{-1/2}$, where $\lambda_e \equiv \hbar/m_e c$ is the electron Compton wavelength. The associated momentum is $p \sim (\hbar/r_{\rm gyr}) \sim m_e c \, (B/B_Q)^{1/2}$.

This shows that electrons gyrate *relativistically* in fields $B > B_Q$. One thus expects excitation energies in excess of $m_e c^2$. This is borne out by the solution to the Dirac equation for an electron in a homogeneous magnetic field. The Dirac spinors are proportional to Hermite polynomials, and the energy levels or "Landau levels" are

$$E_n = \left[m_e^2 + p_z^2 + m_e^2\, n\,(2B/B_Q)\right]^{1/2}, \tag{1}$$

in units with $\hbar = c = 1$ (adopted also in many equations that follow). The first term in the square brackets is the rest energy. The p_z-term gives the energy of motion parallel to the field, which can take a continuum of values. The discrete energy levels are given by $n = 0, 1, 2\ldots$ These states are also eigenstates of spin, with the $n = 0$ ground state always having $s = -\frac{1}{2}$. For $p_z = 0$, the ground state energy is $E_o = m_e$, independent of B. In a semi-classical picture, one could say that the negative spin-alignment energy in the ground state cancels with the zero-point gyration energy. Excited Landau levels are two-fold degenerate in s. The first Landau-level excitation energy is $\omega_B(1) = E_1 - E_o \approx (2B/B_Q)^{1/2}\, m_e$ for $B \gg B_Q$. Because this energy is so large, electrons almost always remain in the ground state for processes thought to occur near the surfaces of ultra-magnetized neutron stars.

Electron *self-interactions* resolve the degeneracies of the Landau levels, and shift the ground state energy. This was first demonstrated by Schwinger, who estimated the "anomalous" magnetic moment of the electron [1]. The relevant Feynman diagram is shown in Figure 1: a free electron (traveling upward on the page) emits a virtual photon, interacts with the magnetic field, then reabsorbs the photon. The electron's effective spin magnetic moment is enhanced by $(1 + \alpha/2\pi)$ to first order in $\alpha = e^2/\hbar c = 1/137$, the fine-structure constant. This results in a ground-state energy shift

$$E_o = m_e\, \left[\, 1 - (\alpha/2\pi)\,(B/B_Q)\,\right]^{1/2}\, . \tag{2}$$

If extrapolated to $B > B_Q$, this formula would imply that the ground-state energy of an electron goes to *zero* at $B = (2\pi/\alpha)B_Q \approx 4 \times 10^{16}$ Gauss. For stronger B, the vacuum would become unstable to pair production, with dramatic astrophysical consequences [2]. But eq. (2) is actually only valid in the sub-B_Q regime. More generally, the electron's self-energy is determined by the sum of Feynman diagrams shown in Figure 2 (ref. [3]). The triple line on the left-hand side represents the physical electron propagator (i.e., the probability amplitude for an electron to move from point A to point B). The double lines on the right are bare propagators for an electron in the presence of a magnetic field, corresponding to basis states

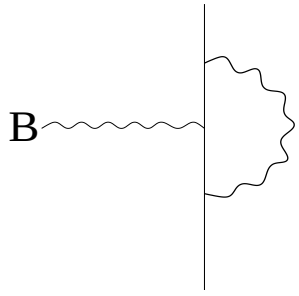

FIGURE 1. Anomalous magnetic moment diagram.

with energies given by eq. (1).[1]

When the calculation is done, it is found that the electron ground-state energy diminishes according to eq. (2) as B increases within the Schwinger domain $B \ll B_Q$, but it reaches a *minimum value* of $(1 - 4.6 \times 10^{-5})m_e$ at $B = 0.25\, B_Q$ and then rises [4,5]. At $B > 0.65\, B_Q$ the electron grows heavier than m_e, but only slowly. The asymptotic fractional enhancement, valid at very large B, is [6]

$$(E_o - m_e)/m_e = (\alpha/4\pi)\left(\left[\ln(2B/B_Q) - \xi - \tfrac{3}{2}\right]^2 + \beta\right) \qquad B \gg B_Q \qquad (3)$$

to first order in α, where $\xi = 0.577$ is Euler's constant, and $\beta \approx 3.9$ is a numerical constant (estimated here from the numerical integrations of ref. [4]).

Thus, an electron's ground-state energy is doubled, $E_o \sim 2m_e$, only at $B \sim 10^{32}$ Gauss. (Higher-order corrections might change this result somewhat.) Of course, the maximum fields attained in neutron stars fall far short of this. The dynamical saturation field for convective motions in nascent neutron stars is $\sim 10^{16}$ G; and $B \sim 3 \times 10^{17}$ G is possible if the free energy of differential rotation in a rapidly-rotating, newborn neutron star is efficiently converted by a post-collapse dynamo [7,8]. But if $B > (8\pi P Y_e)^{1/2} \sim 10^{17}$ G, where P is the pressure and Y_e the electron fraction in the liquid interior of a neutron star, then buoyancy overcomes stable stratification and an inhomogeneous field is dynamically lost [9,8].

For $B \sim 10^{17}$ G, eq. (3) implies $E_o - m_e \approx 0.03\, m_e$. Thus, magnetic self-energy corrections for electrons and positrons are probably not important over the range of magnetic fields and at the level of accuracy typically attained in neutron star astrophysics.

---

[1] Self-interactions also occur when $B = 0$. The double-line propagators of Fig. 2 are then replaced with single-line, free-electron propagators (plane-wave states), and the resultant energy shifts—formally divergent—are absorbed into the electron's known rest mass by the renormalization of quantum electrodynamics. A strong magnetic field changes the self-energy when the same renormalization prescriptions are used. Note that the Schwinger diagram of Fig. 1 is included in the second diagram on the right of Fig. 2: when $B < B_Q$, the double-line propagators can be approximated as single-line, free electron propagators undergoing discrete, perturbative interactions with the magnetic field. Positron intermediate states are included; they correspond to a subset of the vertex time-orderings which are summed over. The lowest-order tadpole diagram gives no contribution in a homogeneous magnetic field.

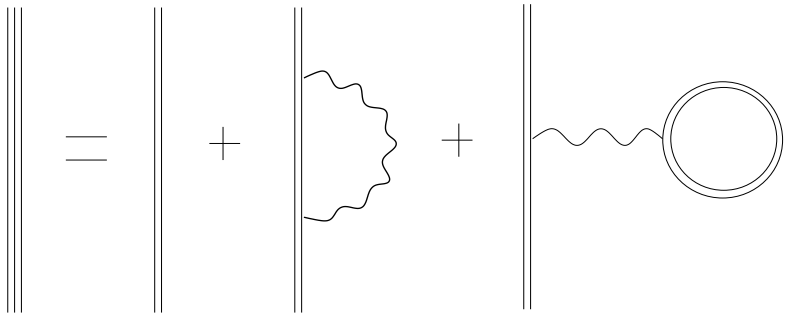

FIGURE 2. Electron self-energy in a magnetic field: lowest-order diagrams.

ATOMS AND MOLECULES AT $B > B_Q$

At sufficiently low temperatures, a magnetar's surface will be covered with atoms and molecules. This surface structure can have consequences for the star's quiescent X-ray emissions, because it determines the work function for removing charged particles from the surface, as necessary for maintaining currents in the magnetosphere [10]. Such currents may result from magnetically-driven crustal deformations such as *twists* of circular patches of the crust.[2] If a bundle of field lines, describing an arch in the magnetosphere, has one footpoint twisted (with the motion driven from below by the evolving field), then a current must flow along the arch to maintain the twisted exterior field, since $\oint \mathbf{B} \cdot \mathbf{d}\ell = 4\pi I/c$. Surface impacts of the flowing charges create hot spots at the arch's footpoints and ultimately dissipate the exterior magnetic energy of the twist, with implications for SGR and AXP X-ray light curves and their time-variations [10]. Here we focus on the atomic and molecular physics that comes into play, following a paper by Ruderman [11] and extending the arguments to $B > B_Q$.

The Bohr radius of a hydrogen atom is $r_o = \lambda_e/\alpha$. The quantum gyration radius, $r_{\rm gyr} = \lambda_e\,(B/B_Q)^{-1/2}$, is smaller than r_o for $B > \alpha^2\,B_Q = 2.4 \times 10^9$ G. This is the characteristic field strength at which magnetism radically alters the atomic structure of matter.[3] At $B > \alpha^2 B_Q$, an atomic electron is constrained to gyrate along a cylinder which lies entirely within the spherical volume that the unmagnetized atom would occupy. Electrostatic attraction binds the electron strongly to the central nucleus. At $B \gg \alpha^2\,B_Q$ the cylinder becomes very long and narrow, and atomic binding energies are adequately given by eigenvalues of the one-dimensional Schrödinger equation. A simple, intuitive estimate—which gives a good estimate of the ground state energy despite its lack of rigor—involves idealizing the atom as a line-charge of length 2ℓ. For linear charge density $e/2\ell$, the electrostatic energy is $\varepsilon = -(e^2/\ell)\ \ln[\ell/\,r_{\rm gyr}]$. A lower cutoff $r_{\rm gyr}$ is necessary because the charge distribution does not resemble a line when you get within $\sim$ $r_{\rm gyr}$ of the nucleus. It is more like a sphere, contributing an energy $\sim -qe/r_{\rm gyr}$ where $q = er_{\rm gyr}/\ell$; but this contribution can be neglected in the limit $\ell \gg r_{\rm gyr}$ or $B \gg \alpha^2 B_Q$. Thus, the ground state energy, including the energy of non-relativistic motion parallel to $\mathbf{B}$, is $\mathcal{E}_o(\ell) = (\hbar^2/2m_e\ell^2) - (e^2/\ell)\,\ln[\ell/\,r_{\rm gyr}]$. Minimizing this according to $d\mathcal{E}_o/d\ell = 0$, we find $\ell \simeq r_o\,[\,\ln(r_o/r_{\rm gyr})\,]^{-1}$. This shows that the *length* of the thin cylindrical atom is less than the Bohr diameter, but only by a modest, logarithmic factor. The ground state hydrogen binding energy is then

---

[2] Crustal twists, with spiral patterns of shear strain, may be a common type of magnetically-driven deformation. The pressure in the crust is due mostly to degenerate particles (relativistic electrons, and free neutrons at densities above neutron drip), but the shear modulus is due only to relatively weak Coulomb forces of the lattice. Hence the crust is relatively incompressible, and pure shear deformations allow the largest range of motion, with the greatest energy transfer between the crust and the magnetic field.

[3] The largest field you are ever likely to encounter personally is $\sim 10^4$ G if you have an medical MRI scan. Fields $\gtrsim 10^9$ G would be instantly lethal.

$$\mathcal{E}_o \simeq -(\epsilon_o/4)\,[\ln(B/\alpha^2\,B_Q)\,]^2 \qquad \text{for} \qquad B \gg \alpha^2 B_Q, \tag{4}$$

where $\epsilon_o = \alpha^2 m_e/2 = 13.6$ eV is one Rydberg. Note that $E \propto [\ln B]^2$ energy scalings are ubiquitous in ultra-magnetized systems (cf. eqs. 3,4,5).

As B increases beyond $B \sim B_Q$, the radius of the atomic cylinder shrinks to less than the Compton wavelength but eq. (4) remains a reasonably good approximation. This is because the electron's inertia for longitudinal motion ($\parallel \mathbf{B}$) stays close to m_e in the ground-state Landau level even at $B > B_Q$. Equation (4) would become invalid if the longitudinal motion became relativistic. But this would require $\ell < \lambda_e$, which occurs only at $B > \alpha^2 \exp(2/\alpha)\, B_Q \approx 10^{115}$ G. Magnetic fields can never get this strong. We will show that the vacuum breaks down at smaller B.

Equation (4) implies that the binding energy of hydrogen near the surface of a magnetar with $B \simeq 10\, B_Q$, is $\mathcal{E}_o \simeq 0.5$ keV. This is comparable to the surface temperatures of some young magnetar candidates [12,13].

There are two classes of *hydrogenic excitations.* Longitudinal excited states are well-approximated as multi-nodal eigenfunctions of the 1-D Schrödinger equation; e.g., the first excited state has a node at the position of the nucleus. Transverse excited states involve transverse displacements of the center of electron gyration away from the nucleus. Semi-classically, the electron then experiences $\mathbf{E} \times \mathbf{B}$ drift, and its center of gyration moves in a circular orbit around the nucleus. (See ref. [11] for details.) Of course, Landau-level excitations are also possible, but the excitation energy is enormous for $B > B_Q$. Atoms generally become unbound when such free energies are present.

Longitudinal excitations tend to require more energy than transverse, so in ultra-magnetized *multi-electron atoms,* orbitals corresponding to transverse hydrogenic states fill up before longitudinal. In fact, for $B > Z^3\alpha^2 B_Q \approx (Z/26)^3\, B_Q$, where Z is the electron number, no orbitals with longitudinal nodes are occupied, and the atomic structure is very simple [11,14]. Note that Fe^{56}, which is likely to be the dominant nuclear species on a clean neutron star surface, has $Z = 26$. Thus, this condition is satisfied on magnetars, but not on radio pulsars with fields $\sim 10^{12}$ G. The atomic binding energy is then

$$\mathcal{E}_o(Z) \simeq -(7/24)\; Z^3\; \epsilon_o\; [\ln(B/Z^3\,\alpha^2\,B_Q)\,]^2. \tag{5}$$

When $B \gg Z^3\alpha^2 B_Q \approx (Z/26)^3\, B_Q$, atoms on a neutron star's surface form long polymer-like molecular chains parallel to $\mathbf{B}$, bound by the electrostatic attraction of shared electrons. The molecular binding energy per nucleus is [11,15,16]

$$\Delta\mathcal{E} \simeq -(3/2)\, Z^3\, \epsilon_o\; (B/Z^3\,\alpha^2\,B_Q)^{0.37}. \tag{6}$$

Together, these results determine the approximate work function for ionic emission from a magnetar's surface [10].

VACUUM POLARIZATION AND RADIATIVE PROCESSES

Photon modes in the magnetized vacuum include the extraordinary mode or *E-mode*, with oscillating electric vector $\mathbf{E_E} \perp \mathbf{B}$, and the ordinary mode or *O-mode*, with $\mathbf{E_O} \perp \mathbf{E_E}$. Both electric vectors are also orthogonal to $\mathbf{k}$, the direction of propagation.[4] Due to the process shown in Fig. 3, where the double-lines are propagators for a magnetized, virtual e^+ e^- pair, the indices of refraction of the two modes are very different at $B > B_Q$: [5]

$$n_O = 1 + (\alpha/6\pi)\ \sin^2\theta_{kB}\ (B/B_Q)$$
$$n_E = 1 + (\alpha/6\pi)\ \sin^2\theta_{kB}.$$

If $n_O - n_E \gtrsim (k\ell_B)^{-1}$, where k is the wavenumber and ℓ_B is the scale-length of variation of the magnetic field, then the modes adiabatically track: E stays E and O stays O as photons move through the changing field geometry. This condition is generally satisfied for X-rays in the magnetospheres of magnetars. Shaviv, Heyl & Lithwick [19] used geometrical optics to model *magnetic lensing* in the vicinity of a magnetar with a pure dipole field and a uniformly bright surface. They found O-mode image distortion and amplification, varying with viewing angle. This remarkable effect may be hard to observe in practice because fields $B \gtrsim (6\pi/\alpha)B_Q \sim 10^{17}$ G are required to produce strong lensing effects. Observations may also be complicated by non-uniform surface brightness, gravitational lensing [20], higher-order magnetic multipoles, photon splitting (see below) and X-ray emission from a magnetar's diffuse, Alfvén-heated halo.

When the excitation energy of the first Landau-level is much greater than the photon energy, $\omega_B(1) \equiv m_e[(1 + 2B/B_Q)^{1/2} - 1] \gg \omega$, then *photon scattering off electrons* is strongly suppressed in the E-mode. Semi-classically, this is easy to understand: the radiation electric field ($\mathbf{E_E} \perp \mathbf{B}$) is unable to significantly drive electron recoil. Paczyński first noted [21] that this greatly accelerates X-

---

[4] Photon eigenmodes are linearly polarized, as described here, except in narrow zones of $\mathbf{k}$-space where the angle between $\mathbf{k}$ and $\pm\mathbf{B}$ satisfies $\theta_{kB} \lesssim (\omega/m_e)^{1/2}\,(B/B_Q)^{-1/2}$ and $\hbar\omega$ is the photon energy. For propagation along $\pm\mathbf{B}$ within these zones, the E and O modes are elliptically polarized; and circularly polarized for $\mathbf{k} \parallel \pm\mathbf{B}$.

[5] The affect of a magnetized *plasma* on the eigenmodes and indices of refraction is small in comparison to the magnetic vacuum polarization so long as $\omega \gg \omega_{c2} \equiv (3\pi/\alpha)^{1/2}\ (B/B_Q)^{-1/2}\ \omega_p$ for $B \gg B_Q$, where $\omega_p = (4\pi N_e e^2/m_e)^{1/2}$ is the plasma frequency and N_e is the electron density (see [18] and references cited therein). This is satisfied in many or most applications to observable phenomena in magnetar magnetospheres since $\omega_{c2} = 0.13\ (N_e/10^{23}\,\mathrm{cm}^{-3})^{1/2}\ (B/10\,B_Q)^{-1/2}$ keV.

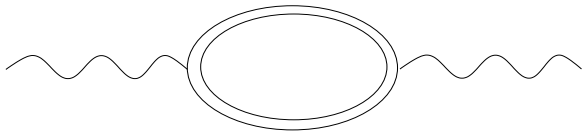

FIGURE 3. Vacuum polarization diagram.

ray diffusion in the vicinity of magnetars, facilitating hyper-Eddington burst and flare emissions. The E-mode scattering cross section, relative to Thomson, is $\sigma(E)/\sigma_T \sim (\omega/m_e)^2\,(B/B_Q)^{-2}$ in the regime of possible relevance for soft gamma repeater (SGR) bursts; see §3.1 of ref. [17] for more details.

Photon splitting and merging, another important radiative effect, is depicted in Figure 4, with time advancing from left to right for splitting, and right to left for merging. These processes are kinematically forbidden in free space, but they operate at $B > B_Q$ because the field acts as an efficient sink of momentum. (Note the double-line, *magnetized* e^- and e^+ propagators in Fig. 4.) The dominant splitting channel is $E \to O\ O$. The rate for $B > B_Q$ and $\omega < m_e$ is [22,23]

$$\Gamma_{\rm sp} = (\alpha^3/2160\pi^2)\ \sin^6\theta_{kB}\ (\omega/m_e)^5\ m_e. \tag{7}$$

(Splitting $E \to O\ E$ also occurs, but at a lower rate.) Note that $\Gamma_{\rm sp}$ increases steeply with increasing photon energy; but it is independent of B for $B > B_Q$. At $B < B_Q$ the process shuts down abruptly: $\Gamma_{\rm sp} \propto (B/B_Q)^6$.

How does this process affect SGR burst spectra? Simple splitting cascade models [24] are illustrative but not realistic since O-mode photons do not split. Realistically, one must consider the subtle interplay of splitting/merging and Compton scattering [17]. In particular, E-mode splitting outside the E-mode scattering photosphere produces O-mode photons which are isotropized by rapid Compton scattering. Subsequent mergers $O\,O \to E$ yield a quasi-isotropic E-mode source function. Only at $B < B_Q$ and outside the O-mode photosphere do the modes truly decouple and all photons stream outward; see §6 of ref. [17] for many more details.

THE ULTRA-MAGNETIZED PAIR GAS

Ultra-strong magnetic fields also have profound *thermodynamic* effects. The magnetized photon-pair gas gives an example. Such a gas may be created during an SGR burst or flare, when a crust fracture or other magnetically-driven instability suddenly injects a large quantity of energy into the magnetosphere [17]. The result is an optically-thick *trapped fireball*, confined by closed field lines, anchored to the star's surface. The gas inside this fireball has remarkable properties, as illustrated in Fig. 5. (This figure is included here courtesy of A. Kudari [25].) The figure shows the ratio of pair energy density to the photon energy density, $\Lambda \equiv U_{e^+e^-}/U_\gamma$,

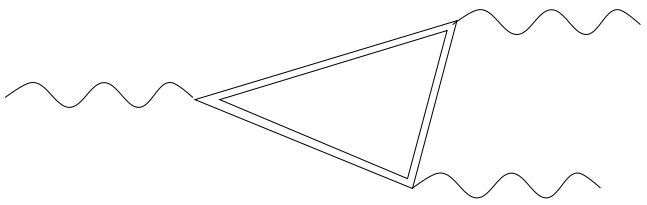

FIGURE 4. Photon splitting and merging in a strong magnetic field.

as a function of T and B. For $T \gg m_e$ and $T \gg \omega_B(1)$, the magnetic field has little effect on the ultra-relativistic pairs: $U_{e^+e^-} = 2 \cdot (7/8) a T^4$, so $\Lambda = (7/4)$. This should hold true across the whole right-hand side of Fig. 5, but only 1000 Landau levels were used in making this graph, so the ratio falls artificially below (7/4) at high T and low B.

The striking peak in Fig. 5 is real, however. It occurs for pairs with non-relativistic longitudinal motion, $T \ll m_e$, and $B > B_Q$. In this regime, only the first Landau level is occupied: $T \ll \omega_B(1)$. The peak occurs because electrons and positrons are strongly localized in directions transverse to the field: $r_{\rm gyr} = \lambda_e \, (B/B_Q)^{-1/2}$. This allows more of them to be packed into a given volume of ultra-magnetized gas. Formulae for thermodynamic parameters of a pair-photon gas in various limits are given in ref. [25] and in §3.3 of ref. [17].

Note that the trapped fireball of a common SGR burst, with energy $\Delta E \sim 10^{41}$ ergs confined within a volume of order $(\Delta R)^3 \sim (10\,{\rm km})^3$ at $B \sim 10\, B_Q$ has a temperature $T \sim 160$ keV [17,25]. This puts it right on the peak in Fig. 5!

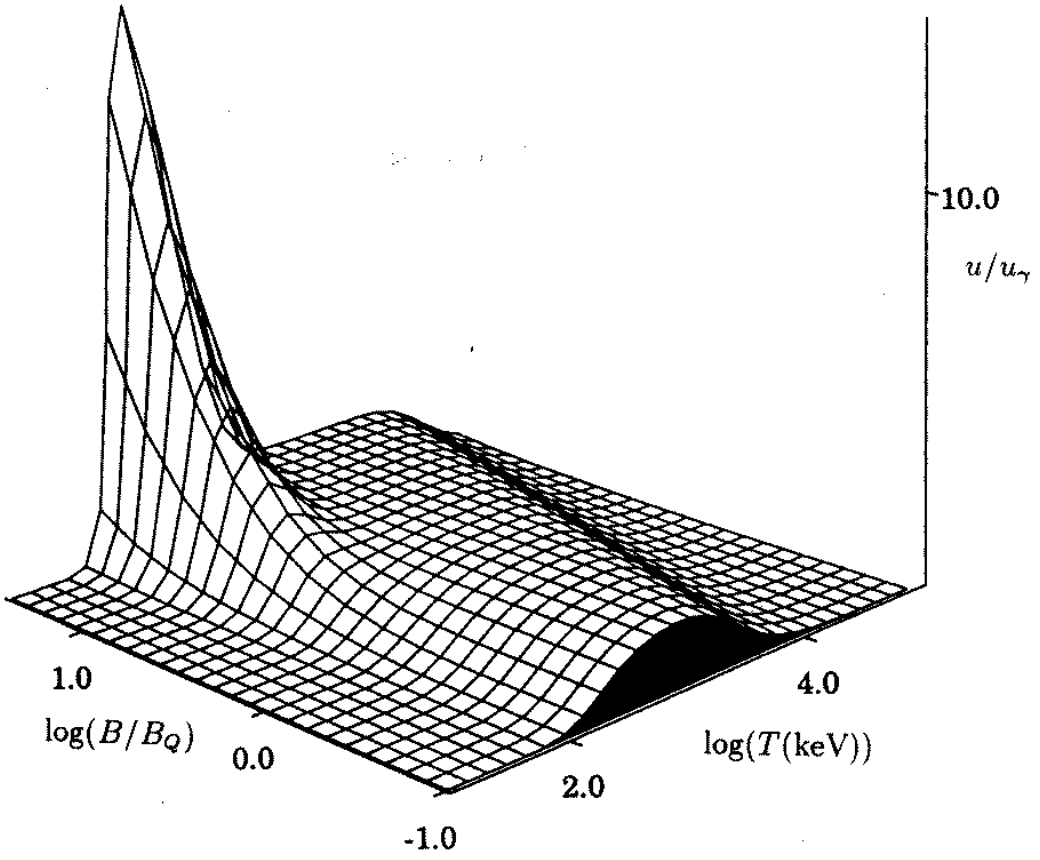

FIGURE 5. The ratio of pair energy density to photon energy density in a pair-photon gas, as a function of temperature and magnetic field strength.

MAGNETIC VACUUM BREAKDOWN

We argued above that a uniformly magnetized vacuum is stable against spontaneous electron-positron pair production. Nevertheless, at sufficiently high B the vacuum must break down. Magnetic monopoles with mass m_η and magnetic charge η are spontaneously created when the energy they acquire in falling across a monopole Compton wavelength, $\varepsilon \sim \eta B \cdot (\hbar/m_\eta c)$, exceeds their rest energy $m_\eta c^2$. Dirac showed that a monopole charge is an integral multiple of $\eta = (\hbar c/2e)$ from the condition that an electron wavefunction must be single-valued in the field of a monopole [26]. Thus, magnetic fields can never get stronger than

$$B_{\rm max} \sim \alpha\ (m_\eta/m_e)^2\ B_Q \quad . \tag{8}$$

A firm upper bound is $B_{max} \simeq 10^{55}$ G for Planck-mass monopoles, $m_\eta = 10^{19}$ GeV. GUT theories predict $m_\eta = 10^{16}$ GeV or $B_{\rm max} \simeq 10^{49}$ G. Superstring/M-theory predicts intermediate values: $m_\eta = \alpha_s^{-1/2} = 10^{17}$–$10^{18}$ GeV, where α_s is the string tension, thus

$$B_{\rm max} \simeq 10^{51} - 10^{53}\ {\rm G}. \tag{9}$$

New work shows that the energy scale for quantum gravity could be as low as $M_o \sim 1$ TeV if there exist "large" extra dimensions to space [27]. The extra dimensions are wrapped in closed geometries (e.g., circles) of size $L \sim 1(M_o/1\,{\rm TeV})^{-2}$ millimeter for two extra dimensions, or $L \sim \ell_p (M_o/M_p)^{-(n+2)/n}\,\ell_p$ for n extra dimensions; where M_p the Planck mass and ℓ_p is the Planck length. This would imply a small limiting field strength: $B_{\rm max} \simeq 10^{23}\,(m_\eta/1\,{\rm TeV})^2$ G. However, there is no experimental evidence for large extra dimensions at the present time. The most plausible upper limit is given by eq. (9).

Thus, *a vast range of tremendous field strengths are possible in Nature.* We don't yet know any objects that generate such fields, but some possibilities have been suggested. For example, superconducting cosmic strings—if they exist—could generate fields $\gtrsim 10^{30}$ G in their vicinities [28]. Perhaps future astrophysicists will regard neutron star magnetic fields as mild!

MAGNETAR SPINDOWN

In this final section, I consider a topic of great current interest, namely recent observations of soft gamma repeater spindown histories [29–34], and their interpretation in the context of the magnetar model. At present, the most promising scenario involves *episodic, wind-aided spindown* (§4 in ref. [10]). This is based upon several background developments. In 1995 Thompson and I proposed that frequent, small-scale fractures in the crust of a young magnetar produce quasi-steady seismic and magnetic vibrations, energizing the magnetosphere and driving a diffuse, relativistic outflow of particles and Alfvén waves (§7.1.2 in ref. [17]). A year later we made a first estimate of this outflow's power [12]. Thompson & Blaes subsequently noted that a magnetar's rate of spindown is greatly accelerated by such a wind

(§VII B in ref. [35]). All of this work pre-dated the discovery of X-ray pulsations from SGRs [29].

How strong is the wind? The wind luminosity, L_W scales roughly with the magnetic energy density in the deep crust,[6] $\propto B_{\rm crust}^2$ [12]. But if $B_{\rm crust} > (4\pi\mu)^{1/2} \sim 6 \times 10^{15}$ G, where μ is the shear modulus in the deep crust, then evolving magnetic stresses overwhelm lattice stresses and the crust deforms plastically instead of fracturing, choking off the Alfvén-powered wind. This suggests an upper limit $L_W \lesssim 5 \times 10^{36}$ erg s^{-1} for a $\sim 10^4$-year-old magnetar [12]. In 1996, we proposed that a wind operating near this upper limit could account for radio synchrotron nebula that seemed to surround SGR 1806−20 [36]. However, we now know that the SGR is not coincident with this nebula [37]. There is no direct observational evidence for a quasi-steady wind from any SGR. Magnetar winds must be mild enough to produce no detected radio emission, with L_W probably much less than the theoretical upper limit of ref. [12], because this limiting value assumed optimal conditions, including the dubious application of a formula at the edge of the regime where it breaks down (i.e., $B_{\rm crust} \sim B_\mu$). It is likely that L_W is comparable to the steady X-ray luminosity emitted by the hot stellar surface and Alfvén-energized halo: $L_W \sim 10^{35}$–10^{36} erg s^{-1}.

Rothschild, Marsden and Lingenfelter have plotted two graphs, included in this volume, which nicely elucidate constraints on SGR spindown for constant L_W and B_{dipole}, based upon formulae derived independently in refs. [38,10].[7] These plots show that wind luminosities $L_W \lesssim 10^{36}$ erg s^{-1} imply $B_{\rm dipole} \gtrsim 10^{14}$ G in order to match the observed values of P and $\dot{P}$; but the implied stellar ages are then moderately shorter than the estimated ages of the putative associated supernova remnants (SNRs). Of course, the SNR associations or ages may be unreliable, since the SGRs lie far from the SNR centers, and the ages are only rough order-of-magnitude estimates. However, we favor a different interpretation: the wind is probably *episodic*, so the effective spindown age of the star is less than the SNR age. In particular, we proposed (in §4.1–4.2 of ref. [10]) that strong winds and rapid spindown prevail only during limited episodes of a young magnetar's life, when it is magnetically active and observable as an SGR. This fits in nicely with observations of anomalous X-ray pulsars (AXPs). These objects have spindown ages $P/2\dot{P}$ that are comparable or *longer* than the ages of their associated SNRs [39,40], suggestive of young magnetars observed during their non-windy, inactive episodes. A fully consistent scenario is possible [10].

Note, incidentally, that $B_{\rm dipole} \lesssim B_Q$ is possible in a magnetar if the lowest-order magnetic moment decays quickly, e.g., via the Flowers-Ruderman instability [41] (see §14.2 and 15.2 in ref. [8]; §7.1.2 in ref. [17]). This is because a magnetar is a *magnetically-powered* neutron star: its emissions depend upon the *total free*

---

[6] Most of the free energy in magnetars is stored in the *internal* magnetic field, probably in toroidal and high-multipole components, so $B_{\rm crust}$ is usually much greater than $B_{\rm dipole}$.

[7] These references correct an inaccuracy in the original wind-aided spindown rate given by ref. [35].

energy and configuration of its magnetic field, not simply upon its exterior dipole moment. The light curve of the 1998 August 27 giant flare gives evidence for strong higher-order multipole moments in SGR 1900+14 [42]. SGR bursts give evidence for magnetically-powered activity (e.g., refs. [17,42–44]).

Marsden et al. [33] also suggested that the spindown rate of SGR1900+14 was enhanced by a factor ~ 2 during the summer of 1998. In the context of the magnetar model, this could mean that L_W increased by a factor ~ 4. Possible evidence for this comes from $\dot{P}$ measurements during RXTE runs immediately preceding and following the interval in question [31]; but it should be noted that RXTE was observing the SGR at those times as a "target of opportunity" because the star was emitting hundreds of bursts [31,34]. Transient accelerated spindown during episodes of vigorous bursting can occur in the magnetar model, because the relativistic outflow may be enhanced. But only a handful of bursts were detected by BATSE during mid-summer of 1998 [34], and the RXTE/ASCA determination of $\dot{P}$ between 1998 Aug. 28 and Sept. 17 was 6.2×10^{-11} s/s [34] (a number that was rounded up to $1. \times 10^{-10}$ in ref. [32]). Furthermore, spindown rates measured over short time intervals, such as during single RXTE runs, can be affected by other transient or periodic effects (e.g., free precession: see §4.3 in ref. [10]; also ref. [45]).

Although an increase in $\dot{P}$ by ~ 2 during the summer of 1998 cannot be ruled out, we suspect that the average spindown rate was similar to that which prevailed at other times during the past few years, and the observed shift in the spindown history was due to an abrupt *spindown glitch* during the extraordinary giant flare of 1998 August 27th. Such a glitch could be caused by the unpinning of crustal superfluid vortices in a magnetar with a crust that has been deformed by evolving magnetic stresses [10].

In conclusion, we have come a long way from the days of ref. [7] when simple magnetic dipole radiation seemed to be an adequate idealization for SGR spindown! More observations are needed to determine whether glitches really occur in SGRs and AXPs [12,46,10] and what sign they may have; whether these stars exhibit free precession (which could give us the first direct measure of a magnetar's *internal* field [45,10]); and to further test and constrain models of these fascinating stars.

Acknowledgments: This work was supported by NASA grant NAG5-8381 and Texas Advanced Research Project grant ARP-028.

REFERENCES

1. Schwinger, J., *Phys. Rev.* **73**, 416L (1948) .
2. O'Connel, R.F., *Phys. Rev. Lett.* **21,** 397 (1968); Chiu, H.Y. & Canuto, V., *Ap.J.* **153**, L157 (1968).
3. Demeur, M., *Acad. Roy. Belg., Classe Sci., Mem.* **28** (1953).
4. Constantinescu, D.H., *Nuclear Phys* **B44**, 288 (1972).
5. Geprägs, R., Riffert, H., Herold, H., Ruder, H. & Wunner, G., *Phys. Rev. D* **49**, 5582 (1994).

6. Jancovici, B., *Phys. Rev.* **187**, 2275 (1969).
7. Duncan R.C., & Thompson C., *Ap.J.* **392**, L9 (1992).
8. Thompson C., & Duncan R.C., *Ap.J.* **408**, 194 (1993).
9. Goldreich P., & Reisenegger A., *Ap.J.* **395**, 250 (1992).
10. Thompson, C., Duncan, R.C., Woods, P., Kouveliotou, C., Finger, M.H. & van Paradijs, J., *ApJ*, submitted, astro-ph/9908086, (2000).
11. Ruderman, M., in *The Physics of Dense Matter*, I.A.U. Symp. No. 53, ed. C.J. Hansen, Reidel, Dordrecht, 1974, pp. 117.
12. Thompson C. & Duncan R.C., *Ap.J.* **473**, 322 (1996).
13. Heyl, J.S. & Hernquist, L., *Ap.J.* **489**, L67 (1997).
14. Lieb, E.H., Solovej, J.P., & Yngvason, J., *Phys. Rev. Lett.* **69**, 749 (1992).
15. Neuhauser, D., Koonin, S.E. & Langanke, K., *Phys. Rev. A* **36**, 4163 (1987).
16. Lai, D., Salpeter, E.E., & Shapiro, S.L., *Phys. Rev. A* **45**, 4832 (1992).
17. Thompson, C., & Duncan, R.C., *M.N.R.A.S.* **275**, 255 (1995).
18. Bulik, T. & Miller, M.C., *M.N.R.A.S.* **288**, 596 (1997).
19. Shaviv, N.J, Heyl, J.S. & Lithwick Y., *M.N.R.A.S.* **306**, 333 (1999).
20. Page, D., *Ap.J.* **442**, 273 (1995).
21. Paczyński, B., *Acta Astron.* **42**, 145 (1992).
22. Adler, S.L., *Ann. Phys.* **67**, 599 (1971).
23. Thompson, C. & Duncan, R.C., in *Compton Gamma-Ray Observatory*, ed. M. Friedlander et al., AIP, New York, 1993, pp. 1085.
24. Baring, M.G., *Ap.J.* **440**, L69 (1995).
25. Kudari, A., Master's Thesis, University of Texas (1996).
26. Dirac, P.A.M., *Proc. Roy. Soc.* **A133**, 60 (1931).
27. Arkani-Hamed, N., Dimopoulos, S., Dvali, G., *Phys. Lett. B* **429**, 263 (1998).
28. Ostriker, J.P., Thompson, C. & Witten, E., *Phys. Lett. B* **180**, 231 (1986).
29. Kouveliotou, C., et al., *Nature* **393**, 235 (1998).
30. Hurley, K., et al., *Ap.J.* **510**, L111 (1999).
31. Kouveliotou, C., et al., *Ap.J.* **510**, L115 (1999).
32. Murakami, T., et al., *Ap.J.* **510**, L119 (1999).
33. Marsden, D., Rothschild, R.E. & Lingenfelter, R.E., *Ap.J.* **520**, L107 (1999).
34. Woods, P., et al., *Ap.J.* **524**, L55 (1999).
35. Thompson, C. & Blaes, O., *Phys. Rev. D* **57**, 3219 (1998).
36. Kulkarni, S., et al., *Nature* **368**, 129 (1994).
37. Hurley, K., et al., *Ap.J.* **523**, L37 (1999).
38. Harding, A.K., Contopoulos, I. & Kazanas, D., *Ap.J.* **525**, L125 (1999).
39. Gotthelf, E.V., Vasisht, G. & Dotani, T., 1999, *Ap.J.* **522**, L49 (1999).
40. Kaspi, V.M., Chakrabarty, D. & Steinberger, J., *Ap.J.* **525**, L33 (1999).
41. Flowers, E. & Ruderman, M., *Ap.J.* **315**, 302 (1977).
42. Feroci, M., et al., *Ap.J.* (2000). [see preliminary paper in these proceedings]
43. Palmer, D.M., *Ap.J.* **512**, L113 (1999).
44. Göğüş, E., et al., *Ap.J.* **526**, L93 (1999).
45. Melatos, A., *Ap.J.* **519**, L77 (1999).
46. Heyl, J.S. & Hernquist, L., *M.N.R.A.S.* **304**, L37 (1999).